Astron. Astrophys. 341, 427–436 (1999)

ASTRONOMY AND ASTROPHYSICS

Detection of moving groups among early type stars

R. Asiain, F. Figueras, J. Torra, and B. Chen

Departament d'Astronomia i Meteorologia, Universitat de Barcelona, Avda. Diagonal 647, E-08028 Barcelona, Spain

Received 14 August 1998 / Accepted 6 October 1998

Abstract. Our procedure to detect moving groups in the solar neighbourhood (Chen et al., 1997) in the four-dimensional space of the stellar velocity components and age has been improved. The method, which takes advantadge of non-parametric estimators of density distribution to avoid any *a priori* knowledge of the kinematic properties of these stellar groups, now includes the effect of observational errors on the process to select moving group stars, uses a better estimation of the density distribution of the total sample and field stars, and classifies moving group stars using all the available information.

It is applied here to an accurately selected sample of early-type stars with known radial velocities and Strömgren photometry. Astrometric data are taken from the HIPPARCOS catalogue (ESA, 1997), which results in an important decrease in the observational errors with respect to ground-based data, and ensures the uniformity of the observed data. Both the improvement of our method and the use of precise astrometric data have allowed us not only to confirm the existence of classical moving groups, but also to detect finer structures that in several cases can be related to kinematic properties of nearby open clusters or associations.

Key words: stars: early-type – stars: fundamental parameters – stars: Hertzsprung–Russel (HR) and C-M diagrams – stars: kinematics galaxy: solar neighbourhood

1. Introduction

The velocity components of early-type stars in the solar neighbourhood are, to a first approximation, normally distributed around those of the circular orbit at the solar position. However, detailed analysis reveals irregularities in these distributions; in other words, certain velocity components are more populated than expected from a gaussian distribution. Such stellar streams were classically referred to as *moving groups* (MG hereinafter). Their consideration as gravitationally unbound systems that share a common origin is controversial, since galactic differential rotation and disk heating efficiently work against their concentration in phase space.

Send offprint requests to: R. Asiain (rasiain@mizar.am.ub.es

Since the appearance of the very first studies outlining the detection of moving groups, their existence has been rather controversial; the restrictive hypotheses adopted and the quality of the data used made it difficult to overcome the problem. In Chen et al. (1997) we presented a moving group detection algorithm based on the analysis of the velocity and age distributions, which used a non-parametric density estimator to avoid any *a priori* knowledge of a moving group's properties, and it was applied to a sample of 1 924 B, A and F main sequence stars, basically extracted from the Hipparcos Input Catalogue (Turon et al., 1992). The velocity components of these stars were determined using ground-based astrometric data from the PPM catalogue (Roser & Bastian, 1991; Roser & Bastian, 1993) and photometric distances. We used stellar age – derived from Strömgren photometry and stellar atmospheric and evolutionary models – since it may be a discriminant variable provided that the moving group's members share a common origin; otherwise, it would not carry additional information, so our results should not be affected when taking it into account. As for age, metallicity could also have been used as a discriminant variable, but, unfortunately, it cannot be derived from photometry for spectral types earlier than $\sim$ A3, and therefore it was an unknown variable for most of our stars (Smalley, 1993).

New contributions to the study of moving groups have appeared since the publication of the precise astrometric data from HIPPARCOS ESA (1997) mission. Sabas (1997) used the SEMMUL algorithm (Celeux and Diebolt, 1986) to decompose the four-dimensional (velocity components and age) density distribution of a sample of 2 578 B5-F5 stars into a sum of gaussians under a maximum likelihood approach, thereby assuming a gaussian profile for a moving group's distribution. In Figueras et al. (1997) we used Sabas (1997) sample of neighbouring stars to determine a moving group's properties through different methods, including Chen et al. (1997), Sabas (1997) and a two and three-dimensional wavelet analysis, which provided an independent non-parametric procedure to detect moving groups. We found a good agreement between the different methods, and the existence of some sub-structures around the Pleiades, Sirius and Hyades classical moving groups' centers. On the other hand, by inspecting – also through a wavelet analysis – the two-dimensional velocity distributions of a sample of A-dwarfs within 125 pc of the Sun, Chereul et al. (1997) found similar

results, i.e. major MGs were sub-structured in a number of tiny velocity clumps. More recently, Dehnen (1998) used the positions, parallaxes, and proper motions of an extended sample (11 865 stars) to estimate the velocity distribution of stars using a maximum-likelihood technique; the study of this distribution allowed this author to detect several MGs.

In this paper we present an improved version of Chen et al.'s (1997) moving group detection algorithm, which uses the three components of the stellar velocity – the U velocity component pointing towards the galactic center, V towards the direction of the galactic rotation and W towards the north galactic pole – and ages. Velocities, computed using the HIPPARCOS catalogue (ESA, 1997) astrometric data, were referred to the heliocentric system and corrected for galactic differential rotation. We dealt with B and A-type stars on the main sequence or in moderately evolved phases (luminosity classes V, IV-V and IV), since they are relatively young stars – ages $\lesssim 10^9$ yr – that, in many cases, are not still in statistical equilibrium, and therefore they can provide information on the conditions in which they were born. Photometric stellar ages in this spectral range can be determined with confidence (Asiain et al., 1997).

The method we present here includes several improvements with respect to the former one, concerning the description of the density distributions, the detection criteria – based now on the effect of observational errors on the density distribution–, and the classification of moving group stars in different streams – performed by considering the distance to the different stellar clumps in our space, instead of a Cluster Analysis.

The steps we followed to construct the stellar sample used throughout this study are described in Sect. 2. In Sect. 3 the details on the moving group detection process are explained, whereas in Sect. 4 we apply it to our sample, evaluate the effect of observational errors, and test the whole procedure. Finally, results are discussed in Sect. 5.

2. Our sample

2.1. Observational data

In order to achieve a good statistical significance in our results we were interested in constructing a sample as extended as possible. For each star in our sample we needed its position, proper motions, radial velocity, distance from the Sun, and Strömgren photometry, used here to determine atmospheric parameters and, from them and by means of stellar atmospheric and evolutionary models, its age.

Astrometric data used in this paper were taken from the HIP Catalogue, which implies an important improvement with respect to ground-based data – as a mean for our stars, HIPPARCOS proper motion errors are more than three times smaller than those in the *Position and Proper Motion* Catalogue (PPM) (Roser & Bastian, 1991; Roser & Bastian, 1993). Radial velocities came from several sources, sorted here by their priority: Barbier-Brossat (1989), observations performed at the *Observatoire de Haute Provence* (France) as a complement to the HIPPARCOS program (e.g. Fehrenbach et al. 1987; Duflot et al. 1992; etc), the HIPPARCOS Input Catalogue (HIC) (Turon et al., 1992), and other miscellaneous sources from the SIMBAD database. Concerning Strömgren photometry, the main sources we used are the Hauck & Mermilliod (1990, 1996) catalogues. In addition, new photometric data for more than 1 200 A-type stars were obtained from an observing program developed by our group since 1988 (Figueras et al., 1991; Jordi et al., 1996; Torra et al., 1998).

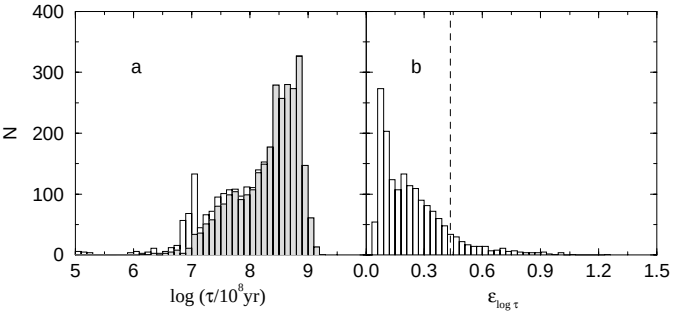

Fig. 1a and b. Distribution of **a** $\log\ \tau$ for the whole sample (*empty histogram*) and for those stars with ϵ_τ/τ <100% (*shadowed histogram*), and **b** $\epsilon_{\log\tau}$. Vertical line in **b** represents 100% error in τ

2.2. Ages and velocities

Stellar ages, and their errors, were interpolated among a set of stellar evolutionary models at a constant metallicity $Z = 0.02$ (Schaller et al., 1992) by using Asiain et al.'s (1997) algorithm, which considers stellar effective temperatures and surface gravities, both derived from Strömgren photometry (Figueras et al., 1991; Jordi et al., 1996), as input parameters. Some restrictions were applied to ensure good ages; namely, our stars were not variables, they had no peculiarities in their spectra nor joint photometry. In Fig. 1, the $\log\ \tau$ histogram of all stars in our sample is shown, along with that corresponding to its error.

We determined the heliocentric velocity components of our stars by considering radial velocities and HIPPARCOS proper motions and parallaxes. Observational errors were propagated taking into account the correlations between HIPPARCOS astrometric parameters – we used an algorithm developed by Meillon et al. (1997).

Additional restrictions were applied in order to avoid high uncertainties in age and velocity; namely, relative error in age $\frac{\epsilon_\tau}{\tau} < 100\%$ (about a 15% of our stars were removed due to this condition); distance from the Sun $<$ 300 pc; relative error in parallax $\frac{\epsilon_\pi}{\pi} < 50\%$. Finally, we eliminated stars belonging to open clusters, in order not to bias our study, as well as a few stars whose velocity referred to Delhaye's centroid – (9,12,7) km s^{-1} – were beyond 65 km s^{-1}, to avoid Population II stars. After this selection, our sample was reduced to 2 061 stars.

We corrected the stellar velocity components for galactic differential rotation (Asiain, 1998), which in fact was a small correction for our stars (its averaged modulus is $\sim$ 2.2 km s^{-1}, with a dispersion $\sim$ 1.7 km s^{-1}), since they are rather close to the Sun. In order to account for any systematic effect introduced

by this correction, the whole moving group detection algorithm was applied to our stars with and without considering it. Results we obtained in both cases were not significantly different. Thus, from now on we only use corrected velocities.

The mean velocity of our total sample was (U,V,W) = (-10.2,-10.3,-7.1) km s^{-1}, a little different from Delhaye's ellipsoid, whereas the mean velocity errors were ($\epsilon_{\rm U}$, $\epsilon_{\rm V}$, $\epsilon_{\rm W}$) = (2.8,2.8,2.2) km s^{-1}, more than 1 km s^{-1} smaller than what we would have obtained from PPM data. By analysing the covariance matrix we determined a mean vertex deviation $\phi = 23\overset{\circ}{.}8 \pm 1\overset{\circ}{.}2$, and a ratio between the velocity dispersions $\sigma_{\rm U} : \sigma_{\rm V} : \sigma_{\rm W}$ = 1: 0.76: 0.50 (with $\sigma_{\rm U} = 16.0$ km s^{-1}). When stars younger than $\sim 10^8$ yr were not considered we obtained $\sigma_{\rm U} : \sigma_{\rm V} : \sigma_{\rm W}$ = 1: 0.66: 0.50.

3. Procedure description

3.1. Density distributions

Most of the published techniques to detect moving groups impose strong assumptions, such as small dispersions in their mean V-velocity component, or the *a priori* knowledge of their mean velocity components. Following Chen et al. (1997), the procedure presented here was designed to use the maximum available information and to avoid preconceptions as far as possible. The only relevant hypothesis we adopted concerns the gaussian nature of the velocity distribution of field stars (Schwarzschild, 1908), which has been demonstrated to provide a good description of the general distribution of neighbouring disk stars.

MGs were detected by assuming that they are responsible for the local irregularities over the smooth field distribution in the four-dimensional space (U,V,W,log τ). In other words, the observed probability density function (*pdf* hereafter) of the total sample ($\rho_{\rm tot}$) is composed of the field star ($\rho_{\rm field}$) and MG member's ($\rho_{\rm MG}$) contributions, i.e.

$$\rho_{\rm tot}(\boldsymbol{x}) = \rho_{\rm field}(\boldsymbol{x}) + \rho_{\rm MG}(\boldsymbol{x}) \, , \tag{1}$$

where $\boldsymbol{x}$ is a vector in the four-dimensional space (U,V,W,log τ) – in fact, each of these coordinates was linearly transformed to make their variances equal to unity (*normalized coordinates*). To describe the observed distribution of the total sample we used a normal kernel probability density function, i.e.

$$\rho_{\rm tot}(\boldsymbol{x}) \; = \; \frac{\Sigma^{-1/2}}{n h_{\rm tot}^d (2\pi)^{d/2}} \times \sum_{i=1}^{n} {\rm e}^{-\frac{1}{2h_{\rm tot}^2}(\boldsymbol{x}-\boldsymbol{x}_i)^T(\Sigma)^{-1}(\boldsymbol{x}-\boldsymbol{x}_i)} \tag{2}$$

where d is the dimension of our variables (=4), n is the number of stars in our sample, $h_{\rm tot}$ a smoothing parameter, (Σ) the covariance matrix, and $\boldsymbol{x}_i$ ($i = 1, \ldots, n$) is the sample set defined in our four-dimensional space. The field distribution function was separated in two independent parts, one accounting for the velocity distribution ($\rho_{\rm v}(\boldsymbol{v})$) and the other for the log τ distribution ($\rho_\tau(\tau)$),

$$\rho_{\rm field}(\boldsymbol{x}) = \rho_{\rm v}(\boldsymbol{v}) \rho_\tau(\tau).$$

As already mentioned, we assumed that $\rho_{\rm v}(\boldsymbol{v})$ followed an ellipsoidal distribution, i.e.

$$\rho_{\rm field}(\boldsymbol{v}) = \frac{1}{\Sigma^{1/2}(2\pi)^{d/2}} {\rm e}^{-\frac{1}{2}(\boldsymbol{v}-\boldsymbol{\mu})^T(\Sigma)^{-1}(\boldsymbol{v}-\boldsymbol{\mu})},$$

where $\boldsymbol{\mu}$ is the mean velocity components vector. As it can be seen in Fig. 1 the log τ distribution is far from being gaussian (as assumed in Chen et al. 1997). To determine $\rho_\tau(\log \tau)$ we applied a kernel *pdf* similar to that given by Eq. 2, with $d = 1$, $h = h_{\rm field}$ and (Σ) = 1.

When using a kernel *pdf* to describe the density distribution of a variable, the window width (or smoothing parameter) h must be carefully selected – small values of h emphasize noisy structures while large h's smooth all the details of the distribution. For a gaussian distribution it can be demonstrated (Silverman, 1986) that the optimum h value is:

$$h_{\rm gau} = \left(\frac{4}{d+2} \right)^{1/(d+4)} n^{-1/(d+4)}.$$

As shown below, the four-dimensional distribution of our total sample had several peaks, which means that a proper $h_{\rm tot}$ to describe such a distribution must be smaller than $h_{\rm gau}$. The log τ distribution of field stars was smoothed to remove all possible "bumps" due to moving groups, so $h_{\rm field} > h_{\rm gau}$. From this point on we adopted the values $h_{\rm tot} = 0.5 \cdot h_{\rm gau}$ and $h_{\rm field} = 1.5 \cdot h_{\rm gau}$. The adoption of a different pair of windows' widths may have important consequences for the main properties of MGs, especially for the velocity dispersions and the number of MG members detected. We will come back to this point in Sect. 4.

3.2. Threshold function

Our method detects MG members by comparing both the total *pdf* ($\rho_{\rm tot}$) with the field one ($\rho_{\rm field}$). In order to avoid the classification of noisy structures as real MGs, the first condition imposed to detect MG stars is:

$$\rho_{\rm tot}(\boldsymbol{x}) - \rho_{\rm field}(\boldsymbol{x}) > \mathcal{C}(\boldsymbol{x}), \tag{3}$$

where $\mathcal{C}(\boldsymbol{x})$ (*Threshold Function*) was determined by recomputing m times (m=100) the density estimator $\rho_{\rm tot}(\boldsymbol{x})$, each time randomly shifting the position of our stars in the space (U,V,W,log τ), once normalized, according to the observational errors[1]. We defined $\mathcal{C}(\boldsymbol{x})$ as the dispersion of this kernel function at the point $\boldsymbol{x}$, i.e.

$$\mathcal{C}(\boldsymbol{x}) = \left[\frac{\sum_{i=1}^{m} \left(\rho_{\rm tot}^i(\boldsymbol{x}) - < \rho_{\rm tot}(\boldsymbol{x}) > \right)^2}{m} \right]^{1/2}.$$

[1] The m new positions of each star follow a normal distribution around the mean values, with dispersions equal to the observational errors

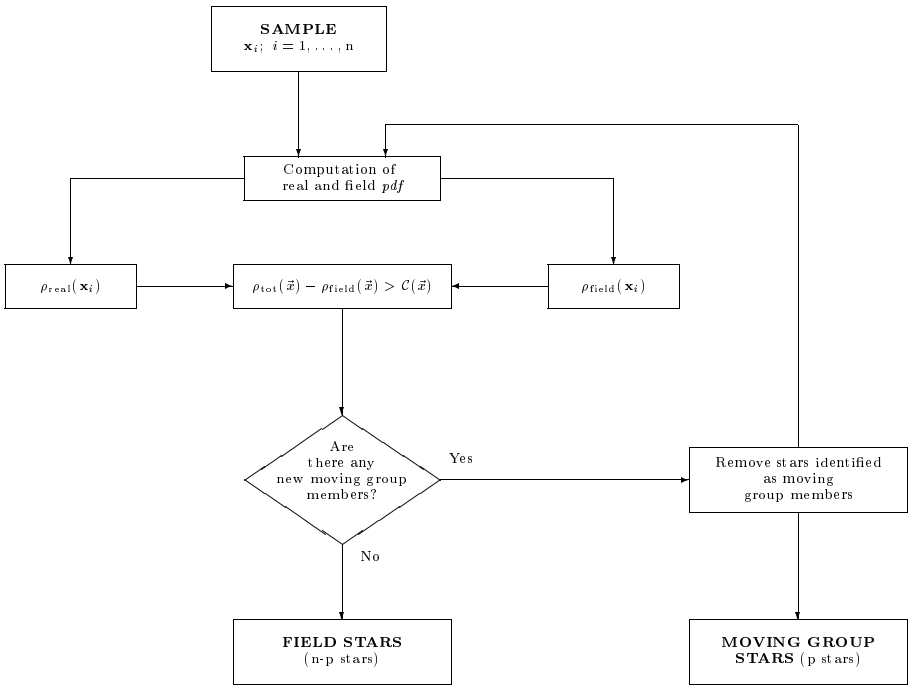

Fig. 2. Moving group detection algorithm flowchart

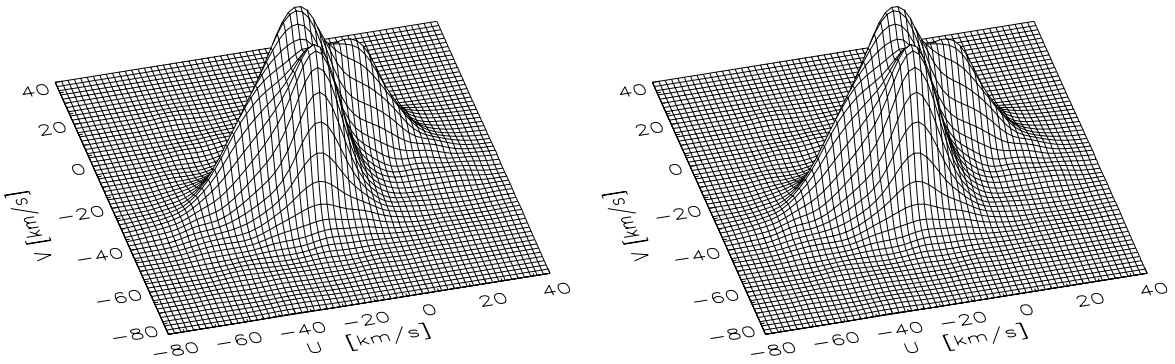

Fig. 3. (U,V) (*left*) and (U,log τ) (*right*) kernel density distribution of the total sample (in this plot $h = h_{\rm gau}$ in order to compare it with the field distribution in Fig. 5)

With this first criterion we select all stars belonging to MGs, but also those field stars sharing the same kinematic and age properties. Only from a statistical point of view we can randomly assign stars to MGs according to the probability

$$\mathcal{P}(\boldsymbol{x}) = 1 - \frac{\rho_{\rm field}}{\rho_{\rm tot}}.$$

This method does not allow us to decide whether a certain star classified as MG really belonged to a moving group or if it was a field star. However, each of these possibilities have a different probability, which is accounted for by $\mathcal{P}(\boldsymbol{x})$ (e.g. stars assigned to MGs that are located at the wings of the $\rho_{\rm tot}$ distribution have a higher probability of being real MG members than those located at its most dense parts). In any case, the mean MG properties are not affected by this assignation procedure.

The procedure is iterated considering the remaining field as the input sample, so a new set of moving group stars is added to the first one, and a new field is obtained. As described in Fig. 2, these iterations are stopped when no new moving group members are found. Finally, moving group stars are separated into different groups, as is described in Sect. 4.2.

4. Application to our sample

In Fig. 3 we show the kernel *pdf* of the total sample in the (U,V) and (U,log τ) planes. Some bumps appear on this distribution nicely located at the position of some nearby open clusters and MGs, as the Pleiades open cluster (Palouš et al., 1977) and Sirius MG (Eggen, 1992a; Eggen, 1996).

In Fig. 4 we show the projection of the function $\mathcal{C}(\boldsymbol{x})$ on the (U,V) plane at a constant W component (= 0 km s^{-1}) and log τ (= 8.5 dex). Empirically we observed a nearly linear relation between ln $\mathcal{C}$ and ln $\rho_{\rm tot}$, i.e.

$$\mathcal{C}(\boldsymbol{x}) = \alpha \rho_{\rm tot}^{\beta}(\boldsymbol{x}), \tag{4}$$

where the fitted values for (α,β) are (0.039,0.47) respectively (correlation coefficient $r = 0.96$). This good correlation was used in further calculations to test the whole method.

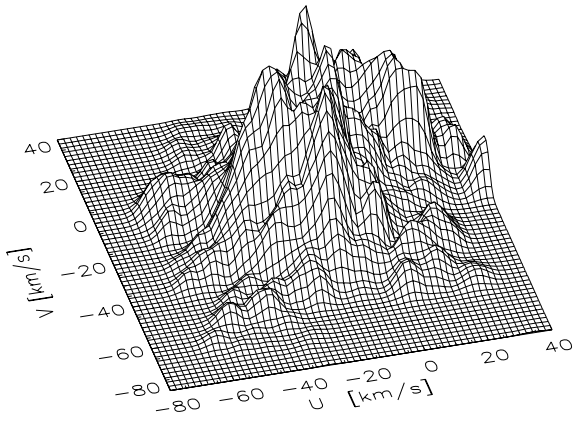

Fig. 4. $\mathcal{C}(\boldsymbol{x})$ in the (U,V) plane, considering a constant value of W and $\log\ \tau$ (0 km s^{-1} and 8.5 dex respectively)

After applying our moving group detection algorithm, our sample was divided in two parts: 574 stars classified as belonging to MGs, and 1487 stars belonging to the field. Five iterations were needed before convergence was achieved. The kernel density functions of both groups of stars are shown in Fig. 5.

4.1. Field stars

The mean field properties did not seem to be significantly affected by the elimination of MG stars. The mean velocity components are now (U,V,W) = (-10.2, -10.8, -7.2) km s^{-1}. With a sample of B, A and F main sequence stars, in Chen et al. (1997) we derived mean velocity components of (-13.4, -11.1, -6.9) km s^{-1}, whereas Sabas (1997), working in a similar spectral range, obtained (-11.5, -14.1, -8.6) km s^{-1}. The difference in our results must be related to the composition of the stellar sample used. The covariance matrix of the field was also very similar to the total sample one, which means that both the velocity dispersions and the vertex deviation did not change significantly once MG stars were eliminated ($\sigma_{\rm U} : \sigma_{\rm V} : \sigma_{\rm W}$ = 1: 0.73: 0.50 with $\sigma_{\rm U} = 17.0$ km s^{-1}; $\phi = 20\overset{\circ}{.}2 \pm 1\overset{\circ}{.}3$). This is not compatible with the suggestion that the vertex deviation in early-type stars is a consequence of the presence of stellar streams in the solar neighbourhood (e.g Mihalas and Binney 1981; Palouš 1986; Dehnen 1998).

We realize that the (U,V) distribution of field stars in Fig. 5 is a gaussian to a first order approximation. A part of the discrepancy with the gaussian distribution comes from the noise allowance introduced by $\mathcal{C}(\boldsymbol{x})$.

4.2. Moving groups

When inspecting the density distribution of MG stars in Figs. 5 and 6 we realized that their typical classification in a few MGs (e.g. Chen et 1997) was only a rough approximation to reality, as suggested by the number of peaks appearing in these figures. Thus, for instance, several maxima in the (U,$\log\ \tau$) plane are centered at the same U component (roughly corresponding to Pleiades open cluster) but correspond to different ages.

To assign MG stars to the different MGs that are observed in Fig. 6 we first determined the kernel *pdf* of these stars and looked for its maxima – a window $h = 0.5 \cdot h_{\rm gau}$ was used in order not to oversmooth this multimodal function. Stars were then assigned to the closest maximum, which was determined by using euclidian distances. This method was performed in both (U,V,W,$\log\ \tau$) and (U,V,$\log\ \tau$) spaces, conveniently normalized to variance unity, thereby evaluating the effect of the third velocity component on this process[2]. Results are given in Tables 1 and 2. Minor groups containing $\approx$ 5% of the MG's stars are not shown in these tables. The significance level of our moving groups was evaluated by comparing the size of irregularities in the four-dimensional kernel *pdf*, due to MGs, with the noise level, by means of the function $\gamma(\boldsymbol{x})$:

$$\gamma(\boldsymbol{x}) = \frac{\rho_{\rm tot}(\boldsymbol{x}) - \rho_{\rm field}(\boldsymbol{x})}{\mathcal{C}(\boldsymbol{x})}.$$

By construction, all the moving group stars fulfilled $\gamma \geq 1$. The maximum value of this function inside a MG ($\gamma_{\rm max}$), given in Tables 1 and 2, was taken here as an indicator of their significance.

MGs were referred to by means of one letter – lowercase when working in four dimensions, and capitals in three dimensions – followed by one number. Those groups sharing similar velocity components were named with the same letter, though different numbers (e.g. a1, a2, etc).

Four-dimensional analysis produced many more groups than the three-dimensional one, as expected. Individual MG's velocity dispersions in 4D were ($\sigma_{\rm U}$, $\sigma_{\rm V}$, $\sigma_{\rm W}$)$\sim$ (4-7,2-6,1-3) km s^{-1}, whereas in 3D ($\sigma_{\rm U}, \sigma_{\rm V}, \sigma_{\rm W}$)$\sim$ (5-6,3-4,2-7) km s^{-1}. The most critical difference concerned the W component, which may be responsible for some doubtful MGs with extremely low $\sigma_{\rm W}$.

In order to evaluate how the adoption of the window's widths $h_{\rm tot} = 0.5 \cdot h_{\rm gau}$ and $h_{\rm field} = 1.5 \cdot h_{\rm gau}$ affected our results, the whole procedure was applied for reasonable combinations of $h_{\rm tot}$ and $h_{\rm field}$, using the three-dimensional analysis to separate MGs; thus, for the determination of the total sample kernel *pdf* (Eq. 2) we considered the values $h_{\rm tot}/h_{\rm gau}$ = 0.3, 0.5 and 0.7, whereas for the field $\log\ \tau$ *pdf* ($\rho_\tau(\log\tau)$), we considered $h_{\rm field}/h_{\rm gau}$ = 1.2, 1.5 and 1.8. We found that the mean velocity components and ages of the most significant groups, along with their dispersions, were not seriously affected by the selection of these h values; differences were < 2 km s^{-1} in the velocity components (but in general $\lesssim 1$ km s^{-1}) and < 1 km s^{-1} in their dispersions, whereas differences in age were $< 5 \cdot 10^7$ yr, and even smaller for its dispersion. The less significant groups, however, appeared as a mixture of those in Table 2. Though $h_{\rm field}$ did not affect the resulting number of moving group members, $h_{\rm tot}$ was critical in this sense. Thus, for $h_{\rm tot}$ = 0.3 $h_{\rm gau}$ we obtained $\sim$ 300 members, whereas for $h_{\rm tot}$ = 0.7 $h_{\rm gau}$ this number increased up to $\sim$ 800 members.

[2] Since the frequency in the vertical motion of disc stars is almost twice the epicycle frequency, unbound systems of stars loose their common W velocity-component in a timescale shorter than that of the other component

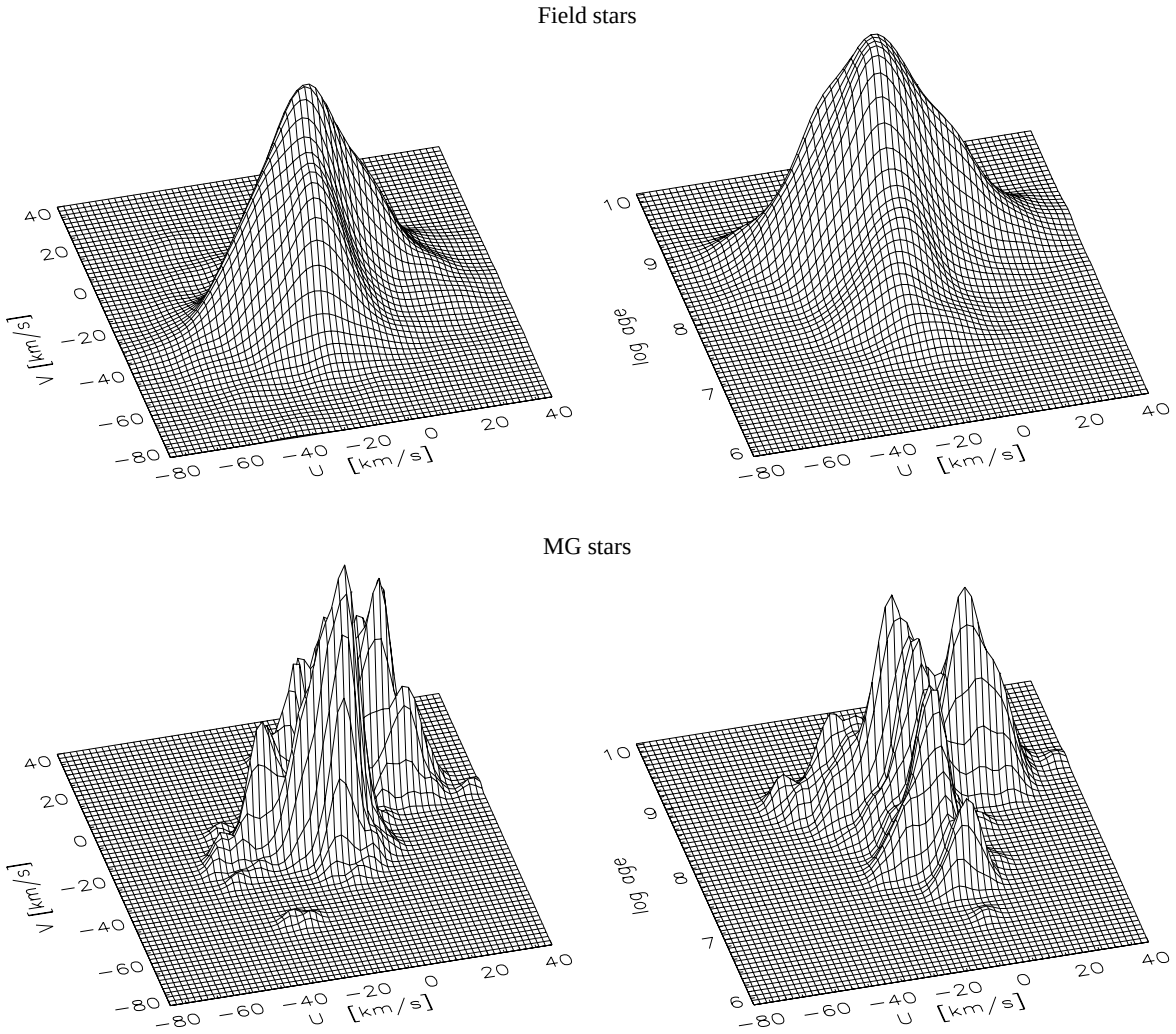

Fig. 5. Kernel *pdf*'s for field stars (*top*) and MG stars (*bottom*) projected on the (U, V) (*left hand*) and (U, $\log\ \tau$) (*right hand*) planes ($h = h_{\rm gau}$ for field stars, and $h = 0.5 \cdot h_{\rm gau}$ for MG stars)

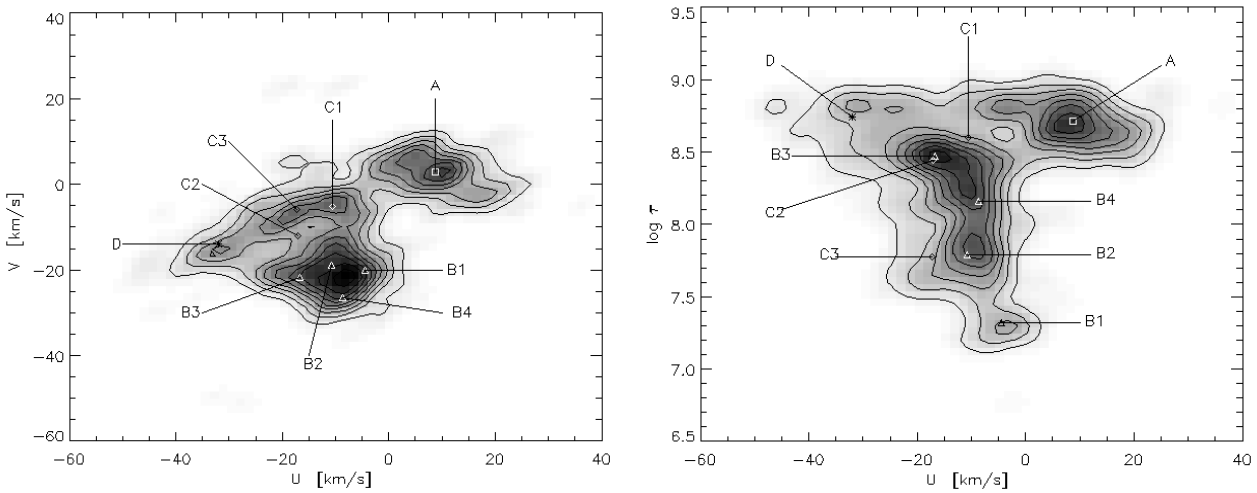

Fig. 6. Kernel *pdf* for MG stars projected on the (U, V) (*left hand*) and (U, $\log\ \tau$) (*right hand*) planes ($h = 0.5 \cdot h_{\rm gau}$). The position of MG centers in Table 2 are also indicated

Table 1. Velocity components and ages (along with their dispersions) and significance level ($\gamma_{\max}$) of the groups found when classifying MG stars in the (U,V,W,$\log\ \tau$) normalized space

Number of members	U [km s^{-1}]	V [km s^{-1}]	W [km s^{-1}]	τ [10^8 yr]	$\gamma_{\max}$	Moving Group
76	$9.2_{(7.0)}$	$2.6_{(4.2)}$	$-8.9_{(1.8)}$	$5.0_{(1.5)}$	5.2	a1
52	$7.5_{(6.4)}$	$3.1_{(3.8)}$	$-1.1_{(3.0)}$	$5.7_{(1.8)}$	4.8	a2
13	$12.3_{(4.4)}$	$-1.2_{(2.4)}$	$-16.3_{(2.9)}$	$4.4_{(1.3)}$	3.2	a3
8	$1.7_{(4.2)}$	$6.6_{(2.0)}$	$-15.9_{(1.3)}$	$5.2_{(0.8)}$	2.7	a4
33	$-4.3_{(4.6)}$	$-20.2_{(3.3)}$	$-5.5_{(1.9)}$	$0.2_{(0.1)}$	7.0	b1
96	$-11.5_{(5.9)}$	$-17.1_{(6.2)}$	$-6.1_{(2.4)}$	$0.6_{(0.2)}$	6.2	b2
80	$-13.4_{(5.2)}$	$-21.6_{(4.7)}$	$-5.7_{(2.5)}$	$2.1_{(0.7)}$	4.2	b3
20	$-8.5_{(6.0)}$	$-26.7_{(5.2)}$	$-13.9_{(2.4)}$	$1.3_{(0.5)}$	3.9	b4
9	$-11.0_{(5.3)}$	$-24.6_{(2.7)}$	$-11.2_{(2.4)}$	$4.5_{(1.8)}$	2.9	b5
54	$-13.4_{(6.4)}$	$-6.4_{(3.7)}$	$-3.3_{(2.7)}$	$3.7_{(1.9)}$	3.3	c1
19	$-15.9_{(4.6)}$	$-0.5_{(4.9)}$	$-9.7_{(1.8)}$	$3.3_{(1.3)}$	3.2	c2
13	$-13.9_{(7.4)}$	$-6.0_{(2.7)}$	$-14.2_{(2.2)}$	$5.4_{(1.2)}$	2.5	c3
7	$-13.6_{(5.2)}$	$-6.1_{(3.3)}$	$-17.0_{(2.0)}$	$1.9_{(0.3)}$	2.1	c4
36	$-30.3_{(5.6)}$	$-14.6_{(3.9)}$	$-0.3_{(3.2)}$	$4.9_{(1.8)}$	3.2	d1
22	$-27.8_{(6.2)}$	$-14.4_{(3.9)}$	$-9.6_{(2.2)}$	$4.1_{(1.8)}$	3.0	d2
6	$-43.1_{(2.4)}$	$-18.4_{(2.7)}$	$-9.2_{(1.3)}$	$6.6_{(1.5)}$	2.3	d3

Table 2. Same as Table 1, working now in the (U,V,$\log\ \tau$) normalized space

Number of members	U [km s^{-1}]	V [km s^{-1}]	W [km s^{-1}]	τ [10^8 yr]	$\gamma_{\max}$	Moving Group
148	$8.7_{(6.6)}$	$2.8_{(4.1)}$	$-6.9_{(5.8)}$	$5.2_{(1.6)}$	5.2	A
34	$-4.5_{(4.7)}$	$-20.1_{(3.3)}$	$-5.5_{(1.9)}$	$0.2_{(0.1)}$	7.0	B1
75	$-10.7_{(5.3)}$	$-18.8_{(3.7)}$	$-5.6_{(2.2)}$	$0.6_{(0.2)}$	6.2	B2
50	$-16.8_{(5.1)}$	$-21.7_{(2.7)}$	$-5.6_{(4.6)}$	$3.0_{(1.2)}$	4.2	B3
53	$-8.7_{(4.8)}$	$-26.4_{(3.3)}$	$-8.5_{(4.7)}$	$1.5_{(0.5)}$	3.9	B4
62	$-10.5_{(5.0)}$	$-5.0_{(2.6)}$	$-7.5_{(6.0)}$	$4.0_{(2.0)}$	3.1	C1
48	$-17.1_{(5.6)}$	$-12.0_{(3.4)}$	$-5.7_{(4.3)}$	$2.8_{(1.2)}$	3.3	C2
22	$-17.4_{(6.1)}$	$-5.9_{(5.8)}$	$-10.0_{(4.7)}$	$0.6_{(0.2)}$	3.4	C3
55	$-32.0_{(6.0)}$	$-14.0_{(4.2)}$	$-6.0_{(6.7)}$	$5.6_{(1.7)}$	3.2	D

4.3. The effect of observational errors

We were interested in quantifying the effect of the observational uncertainties on the MG mean properties. With this purpose we created $\mathcal{N}$ (=25) "copies" of our sample by randomly shifting each star's observed parameters – parallax, proper motions, radial velocity, position and age – around their actual values according to the observational errors.

Our algorithm was applied to the sample's copies, thereby producing $\mathcal{N}$ samples of the MG's members; each of these samples were separated into different MGs in the three-dimensional (normalized) space (U,V,$\log\ \tau$). Not all the groups obtained with each sample's copy could be identified with those in Table 2. The most populated MGs – groups A, B1, B2, C1 and D – appeared in all the copies. By considering the $\mathcal{N}$ copies of each of these MGs, we determined their averaged velocities, ages, and their dispersions, which were almost identical to those in Table 2, as well as the dispersions around these averaged values. These last dispersions, which are a consequence of the observational errors, were $\lesssim 2.5$ km s^{-1} in U and V, and $\lesssim 1$ km s^{-1} in W, much smaller than the mean intrinsic dispersions. It was also found that the contribution of the observational errors to the dispersion in age was smaller than 30%.

In most copies we also obtained a group whose kinematics and age (and also their dispersions) resembled those of B3, except for its U-component, which is -13.2 km s^{-1}, and the number of components, 77 (closer to b3). In only one third of the copies we detected a small group centered at (-41.9,-18.4,-6.6) km s^{-1} and aged $6.6{\cdot}10^8$ yr, which is very similar to "d3", identified with the Hyades MG.

4.4. Testing the procedure

In order to test our procedure as a whole, we generated a sample whose properties were close to the real sample ones, that is to say, a field sample with 1487 stars following, for simplicity, a four-dimensional gaussian – three velocity components and $\log\ \tau$ – with mean velocity components, mean age and covariance matrix equal to those corresponding to the field; each moving group also followed a four-dimensional gaussian distribution with properties taken from Table 2.

The effect of possible noise was accounted for by Eq. 3, where $\mathcal{C}(\boldsymbol{x})$ was estimated by means of expression 4. Once our moving group detection algorithm was applied to the simulated sample, we found 1704 field stars, with velocity components (-10.3,-10.6,-7.2) km s^{-1} (dispersion ratios $\sigma_{\rm U} : \sigma_{\rm V} : \sigma_{\rm W}$ = 1: 0.67: 0.49, and $\sigma_{\rm U} = 16.7$ km s^{-1}) and $\log\ \tau$= 8.4 dex ($\sigma_{\log \tau}$ = 0.4 dex), which are, except for the number of stars, in perfect agreement with the original values.

Furthermore, MG mean velocities and ages, found by means of the three-dimensional analysis, were quite similar to those obtained from real data, the differences in velocity components being $\lesssim 2$ km s^{-1}. However, the number of MG members significantly decreased in all cases, due to the use of the function $\mathcal{C}(\boldsymbol{x})$. This means that in the real case we are under-estimating the number of MG stars, specially for those MG located around the field center, for which $\mathcal{C}(\boldsymbol{x})$ takes its highest values.

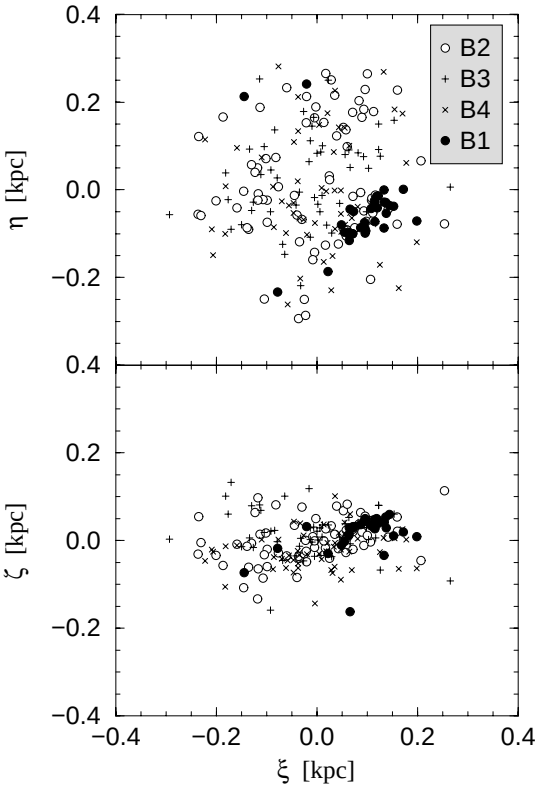

Fig. 7. Position in the Galactic and meridional planes of the Pleiades sub-groups found using the three-dimensional analysis to separate groups. The coordinate system used here is centered on the Sun, with ξ increasing towards the center of the Galaxy, η towards the galactic rotation, and ζ towards the north galactic pole

5. Discussion

Most of the MGs listed in Tables 1 and 2 show kinematic properties that are similar to the classical MG's and to those of some nearby open clusters. Next we analyse such similarities, and compare our results with some recent studies.

Groups named "a" or "A" have a positive U component, and their kinematics resemble that of the classical Sirius MG – see Eggen (1996), Palouš and Hauck (1977), Soderblom & Mayor (1993) and Dehnen (1998). They contain roughly a 30% of the whole MG stars, which are distributed in four sub-structures when working in four dimensions; some of these structures were also reported by Sabas (1997) and Figueras et al. (1997). As it can be seen in Fig. 6, the Sirius MG (indicated by the label "A") is quite extended, which suggests it is composed of several subgroups. The age of these structures is $\approx 5 \cdot 10^8$ yr, in perfect agreement with those determined by Eggen (1996), Palouš & Hauck (1977), Sabas (1997), and Figueras et al. (1997), and only slightly bigger than recent estimations of the Ursa Major cluster's age (the nucleus of Sirius MG), i.e. $3{\cdot}10^8$ yr as found by Soderblom & Mayor (1993), or $4{\cdot}10^8$ yr according to Eggen (1996).

A second family of groups was labeled "b" or "B", and its velocity components are close to Pleiades open cluster ones, so they all are often referred to as the Pleiades MG. In both the three and four-dimensional analysis this structure is mainly composed of four sub-groups (especially well separated in age, as it can be seen in Fig. 6), spatially distributed as shown in Fig. 7 (most of these stars lie on the Goult Belt). The most significant and youngest sub-group, "b1" or "B1", has small velocity dispersions, and it is the only one that is concentrated in space (full circles in Fig. 7). 25 of these stars ($\sim$ 75%) were identified as members of the Scorpio-Centaurus OB association by de Geus et al. (1989), and most of the rest are located around this association. They occupy an elongated volume that is inclined $\sim 40^\circ$ with respect to the direction of the Galactic rotation, and $\sim 20^\circ$ with respect to the galactic plane.

A second sub-group, "b2" or "B2", is the most populated one. Its (U,V) components and age are compatible with those of α Persei – this open cluster has a velocity components (-10.8, -20.5, -0.7) km s^{-1} (Palouš et al., 1977) and an age of $5 \cdot 10^7$ yr (Mermilliod et al., 1997) – and it is also similar to the Pleiades MG as found by Eggen (1992b), (-11.6,-20.7,-10.5) km s^{-1}, or the "A" group of Sabas (1997), i.e. (-10.1,-23.2,-5.3) km s^{-1}.

There are small differences between sub-structures "b3" and "B3", not only concerning the number of members, but also the U velocity component and the age. Though "b3" is also close to the Pleiades MG (e.g. Eggen 1992b, Dehnen 1998), and is in perfect agreement with the results of Chereul et al. (1997), this group is much older than the Pleiades open cluster ($1 \cdot 10^8$ yr, Mermilliod 1997). However, Eggen (1992b) pointed out that the Pleiades MG appears to cover the age range $6 \cdot 10^6$ yr to $2 \cdot 10^8$ yr. On the other hand, the (U,V) components of "B3" are centered near the position of the Puppis MG (Roser & Bastian, 1994), i.e. (-21,-20,-14) km s^{-1} (see Fig. 6). Nevertheless, both

its W component and its age – estimated to be $\lesssim 2 \cdot 10^7$ yr – are quite different from our "B3" group ones (moreover,"B3" stars are not spatially concentrated, in contrast with the Puppis MG members).

Structures "b4" and "B4" are very similar, excepting the W-component and velocity dispersions. Their kinematics and ages are quite close to the Pleiades open cluster ones, i.e. (-5.8,-24.0,-12.4) km s^{-1} (Palouš et al., 1977) and $1 \cdot 10^8$ yr– this age is close to the time elapsed since the passage of the LSR through the center of the Sagittarius spiral arm (e.g. Comerón et al. 1994).

The U and V velocity components and ages of groups "c1", "c3" and "C1" are very similar to group "D" found by Sabas (1997), i.e. (-12.5,-6.2,-8.3) km s^{-1} and $3.2 \cdot 10^8$ yr (their "D" group is probably a mixture of our "c" groups), and to one of the MGs detected by Dehnen (1998), i.e. (-10,-5,-8) km s^{-1}, associated by the authors to the "Coma Berenices" open cluster – nontheless this open cluster has velocity components (-1.8,-8.2,-0.7) km s^{-1}(Palouš et al., 1977). In fact, the (U,V) velocity components of these MGs are very close to those of the Cassiopea-Taurus association, i.e. (U,V)=(-9.9,-6.1) km s^{-1} (Comerón, 1992), though their ages are completely different (it would be more appropriate to name it as the Cas-Tau MG, rather than Coma Berenices MG).

The velocity components of "C2" are closer to those of the IC 2391 open cluster, (-18.3,-13.5,-5.9) km s^{-1}, than Eggen's (1991) IC 2391 MG were. Its age, however, is too large compared with the open cluster age, $3 \cdot 10^7$ yr (Mermilliod et al., 1997), but compatible with Eggen's IC 2391 MG age, 0.8-$2.5 \cdot 10^8$ yr.

Groups "d1", "d2" and "D" have a very large negative U component, though not so much as the Hyades open cluster. Similar groups were reported by Sabas (1997) and Figueras (1997), but they do not seem to be related to any nearby open cluster. The small group "d3" has a velocity vector and age that are very similar to the Hyades open cluster, i.e. (-41.7,-19.2,-1.1) km s^{-1} (Palouš et al., 1977; Perryman et al., 1998) and $6.3 \cdot 10^8$ yr (Mermilliod et al., 1997; Perryman et al., 1998). The low number of members in "d3" may be due to the fact that this MG is not well represented in the spectral type range we considered.

6. Conclusions

Our method to detect moving groups among solar neighbourhood stars was applied to a sample of early-type stars, for which good determinations of (photometric) ages, (trigonometric) distances, and spatial velocities were available. We used a non-parametric approach (a gaussian kernel density estimator) to describe the density distribution of the variables involved in our analysis, i.e. the three components of velocity (in the heliocentric system corrected for differential rotation) and age. Unlike previous studies, we did not impose any "a priori" knowledge on the velocity or age distribution of moving groups.

Local density irregularities over the smooth field distribution were identified as moving groups, and then separated into different groups by linking each star to the closest density distribution maximum in both the (normalized) spaces (U,V,$\log\ \tau$) and (U,V,W,$\log\ \tau$). In this way we found several structures, most of them being compatible with classical moving groups, although we clearly detected substructures inside these groups.

In order to avoid noisy structures, we defined a *Threshold Function* that accounted for the effect of observational errors on the density distribution function. By construction, the moving groups we found were beyond the "noise level" introduced by this *Threshold Function*. The sizes of the irregularities in the field density distribution due to moving groups were $\sim$ 3–7 times greater than the noise, which clearly proves the presence of these moving groups among the early-type stars.

We also evaluated the way in which observational uncertainties were affecting our results by randomly shifting each star's observed parameters around their actual values according to their observational errors. We then applyed our algorithmm to the new samples generated in this way, and found that we could recover most of the main groups. On the other hand, we generated a sample of field and moving group stars with similar properties to those found with the real sample to test the whole moving group detection algorithm; after applying our algorithm, the resulting field and moving group's properties were fairly similar to those obtained from real data. However, the number of moving group's members significantly decresed due to the use of the *Threshold Function*.

Moving group velocity dispersions were large compared with classical results, which cannot be explained from either the detection algorithm itself (it may account only for ~ 2 km s^{-1}) or propagation of the observational errors ($\lesssim 2.5$ km s^{-1}). We are led to consider that moving groups can survive even though their V velocity component does not have a very small dispersion.

In a future paper we will describe how a moving group's properties help us in the study of its origin, its evolution in phase space, and its persistence over time in spite of the effect of galactic differential rotation and disc heating.

Acknowledgements. This work was supported by the CICYT under contract ESP97-1803 and by the PICS programme (CIRIT).

References

Asiain R., Torra J., Figueras F., 1997, A&A 322, 147
Asiain R., 1998, PhD Thesis, Universitat de Barcelona, Spain
Barbier-Brossat M., 1989, A&AS 80, 67
Celeux G., Diebolt J., 1986, Revue de Statistiques Appliquées Vol. XXXIV, n.2
Chen B., Asiain R., Figueras F., Torra J., 1997, A&A 318, 29
Chereul E., Crézé M., Bienaymé O., 1997, Hipparcos – Venice'97, ESA SP-402, p. 545
Comerón F., 1992, PhD Thesis, Universitat de Barcelona
Comerón F., Torra J., Gómez A.E., 1994, A&A 286, 789
Duflot M., Fehrenbach Ch., Mannone C., Burnage R., Genty V., 1992, A&AS 94, 479
Dehnen W., 1998, AJ, in press
Eggen O.J., 1991, AJ 102, 2028
Eggen O.J., 1992a, AJ 104, 1493

Eggen O.J., 1992b, AJ 103, 1302
Eggen O.J., 1996, AJ 112, 1595
ESA, 1997, The Hipparcos Catalogue. ESA SP-1200 (vol I-XVII)
Fehrenbach Ch., Burnage R., Duflot M., et al., 1987, A&AS 71, 263
Figueras F., Torra J., Jordi C., 1991, A&AS 87, 319
Figueras F., Gómez A.E., Asiain R., et al., 1997, Hipparcos – Venice'97, ESA SP-402, p. 519
de Geus E.J., de Zeeuw P.T., Lub J., 1989, A&A 216, 44
Hauck B., Mermilliod M., 1990, A&A 86, 107
Hauck B., Mermilliod M., 1996, private communication
Jordi C., Figueras F., Torra J., Asiain R., 1996, A&AS 115, 401
Meillon L., Crifo F., Gómez A.E., Udry S., Mayor M., 1997, Hipparcos - Venice'97, ESA SP-402, p. 591
Mermilliod J.-C., Turon C., Robichon N., Arenou F., Lebreton Y., 1997, Hipparcos – Venice'97, ESA SP-402, p. 643
Mihalas D., Binney J., 1981, Galactic Astronomy. W.H Freeman and Company, New York
Palouš J., Ruprecht J., Dluzhnevskaya O.B., Piskunov T., 1977, A&A 61, 27
Palouš J., Hauck B., 1986, A&A 162, 54
Perryman M.A.C., Brown A.G.A., Lebreton Y., et al., 1998, A&A 331, 81
Roser S., Bastian U., 1991, PPM Star Catalogue North Vols. 1 & 2. Spektrum Akademischer Verlag, Heidelberg
Roser S., Bastian U., 1993, PPM Star Catalogue North Vols. 3 & 4. Spektrum Akademischer Verlag, Heidelberg
Roser S., Bastian U., 1994, A&A 285, 875
Sabas V., 1997, PhD Thesis, Observatoire de Paris
Schaller G., Schaerer D., Meynet G., Maeder A., 1992, A&AS 96, 269
Schwarzschild K., 1908, Akad. Wissenschaft Göttingen Nach., 191
Silverman B.W., 1986, In: Chapman, Hall (eds.) Density estimation for statistics and data analysis. Arrowsmith Ltd, Bristol
Smalley B., 1993, A&A 274, 391
Soderblom D.R., Mayor M., 1993, AJ 105, 226
Torra J., et al., 1998, A&AS, in preparation
Turon, et al., 1992, The Hipparcos Input Catalogue, ESA SP-1136